DNA Nanotechnology

DOI: 10.1002/anie.200703741

Templated Synthesis of Highly Stable, Electroactive, and Dynamic Metal–DNA Branched Junctions**

*Hua Yang and Hanadi F. Sleiman**

DNA has recently emerged as a promising template to create nanostructures with precisely programmed features.[1] Typical approaches involve the assembly of branched units containing unmodified oligonucleotides.[1,2] In contrast, the incorporation of transition metals into the vertices of DNA nanostructures is much less explored.[3] This is despite the tremendous potential of metals to influence both the function of DNA nanostructures, through their redox, photophysical, magnetic, and catalytic properties, as well as the structure of DNA nanoassemblies, through the plethora of geometries and coordination numbers available to them.[3–9] The development of metal–DNA nanostructures is currently hampered by the need to use metals that are kinetically inert, resist the harsh conditions of oligonucleotide solid-phase synthesis, and do not preferentially bind or react with the DNA bases or phosphate backbone.[3] Furthermore, the limited examples of metal–DNA nanostructures have contained metal centers separated by DNA double strands, which reduces metal-metal interactions.[3] In order to harness the potential of transition metals as functional corner units in DNA assembly, a more systematic approach that bypasses these limitations is necessary.

Herein, we present a template approach that allows for the incorporation of normally labile metal centers, such as copper(I), copper(II), and silver(I), into DNA branch points (Scheme 1a). Remarkably high structural stability and chirality transfer to the metal complex are demonstrated. Moreover, we have used this approach to generate the first example of a dynamic multimetallic metal–DNA assembly, with three metal complexes as the corners, single-stranded DNA as the sides, and multiple DNA double strands at the periphery (Scheme 1d). We demonstrate quantitative and reversible structural switching of these metal–DNA nanostructures by adding specific DNA strands, resulting in controlled modulation of the metal–metal distances. This contribution thus allows the programmable generation of structurally dynamic multimetallic metal–DNA assemblies, with anticipated applications in nanoelectronics, nanooptics, artificial photosynthesis, high-density data storage, and catalysis.

[*] H. Yang, Prof. H. F. Sleiman
Department of Chemistry, McGill University
801 Sherbrooke Street West
Montreal Quebec H3A 2K6 (Canada)
Fax: (+1) 514-398-3797
E-mail: hanadi.sleiman@mcgill.ca

[**] NSERC, CFI, CSACS, CIFAR. H.F.S. is a Cottrell Scholar of the Research Corporation

Supporting information for this article is available on the WWW under http://www.angewandte.org or from the author.

To create stable and electroactive metal–DNA junctions, we examined the attachment of the ligand bis(2,9-diphenyl)-1,10-phenanthroline (dpp) to DNA (Scheme 1a). This ligand has been used by the groups of Sauvage and others to generate interwoven structures.[10] It forms complexes such as $[Cu(dpp)_2]^+$, whose redox potential falls within the compatible window for DNA bases (+0.8 to −0.7 V vs. saturated calomel electrode, SCE),[11] and evidence of partial intercalation of these complexes into DNA has been provided.[12] An ethylene glycol substituted, monotritylated phosphoramidite derivative of dpp was thus synthesized (Scheme 1b, dpp vertex).[13,15] The resulting molecule can be incorporated at any position of a DNA strand using standard solid-phase DNA synthesis, allowing for in-strand complexation of metal centers.

To introduce labile metal centers into DNA vertices, we examined the use of DNA strands as templates to bring two dpp units into close proximity (Scheme 1a). To realize this approach, two complementary 10-mer DNA strands (**1** and **1′**) terminated with dpp at their 5′ and 3′ ends were synthesized. Hybridization of **1** and **1′** and subsequent addition of 1.1 equivalents of either Cu^+, Cu^{2+}, or Ag^+ resulted in quantitative formation of the metal$(dpp)_2$–DNA junctions **2**·Cu^I, **2**·Cu^{II}, and **2**·Ag^I (Scheme 1a, Figure 1a). Denaturation of the DNA arms of these junctions resulted in a single electrophoresis band of significantly lower mobility than **1** and **1′**, showing that the new compounds are held together by metal coordination (Figure 1a). In contrast, untemplated complexation, by incubation of **1** or **1′** separately with these metals, was not possible.[14,15] The structures of **2**·Cu^I, **2**·Cu^{II}, and **2**·Ag^I were confirmed by MALDI-TOF mass spectrometry and spectroscopic experiments.[15] Notably, complexation of the normally five-coordinate Cu^{II} center is shown by its green color and UV/vis bands typical of $[Cu(phen)_2]^{2+}$, while the pink-red Cu^I–DNA complex has a spectrum typical of $[Cu(phen)_2]^+$ and shows fluorescence at 405 nm upon excitation at 330 nm in aqueous solution.[15]

Interestingly, the resulting metal–DNA junctions show dramatically enhanced stability (Figure 1b). While the melting temperature (T_m) of ligand-appended dpp–DNA helix **2** is slightly higher (52 °C) than an unmodified duplex (43 °C), silver coordination increases the T_m to 64 °C, and the T_m of **2**·Cu^I is as high as 80 °C (Figure 1b).[16] This increase is one of the highest reported in melting temperature (+37 °C for a 10-mer) for an appended metal–DNA complex[17] and suggests significant stabilization of the DNA base stack through interaction with the metal unit.

Circular dichroism (CD) spectroscopy of the metal$(dpp)_2$–DNA junctions suggests chirality transfer from DNA to the metal unit (Figure 1c,d). Without metal coordination, the CD

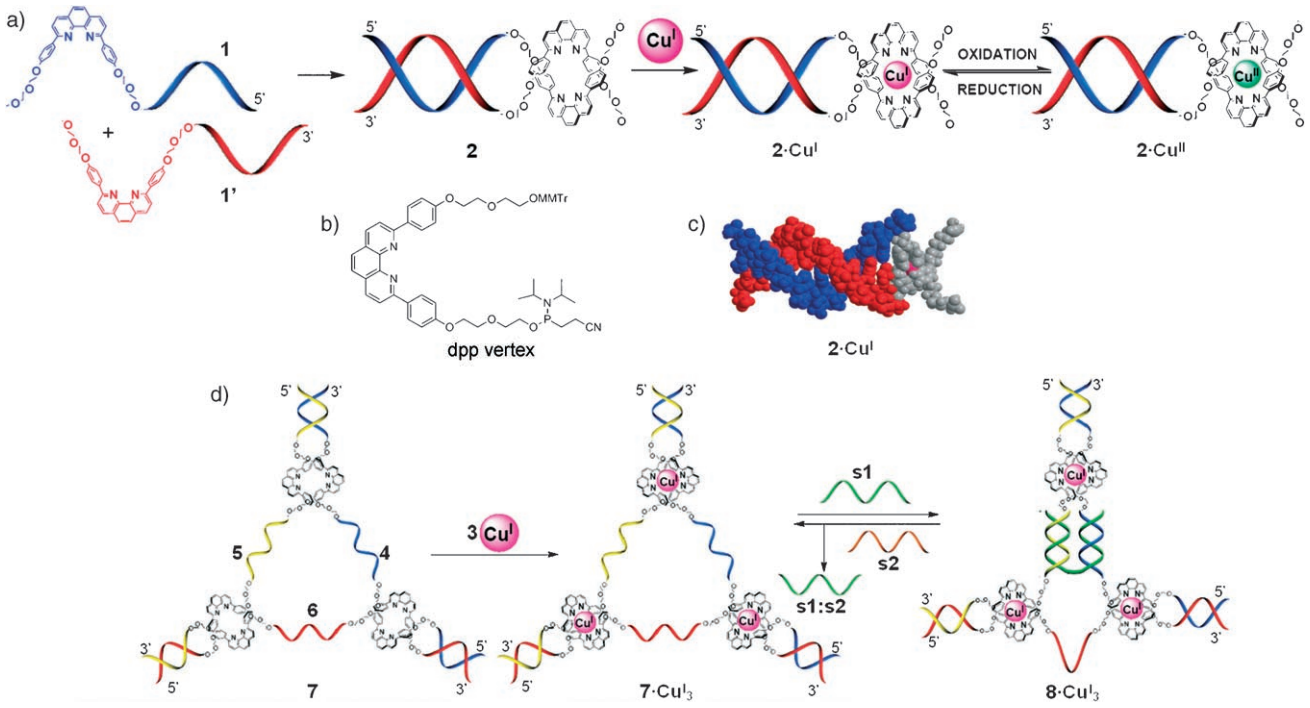

Scheme 1. a) dpp–DNA **1** and **1′** hybridize to form **2**; **2** reacts with Ag^{I}, Cu^{II}, or Cu^{I} to form complexes **2**·Ag^{I}, **2**·Cu^{II}, or **2**·Cu^{I}; **2**·Cu^{I} is oxidized to **2**·Cu^{II} by I_2/H_2O; **2**·Cu^{II} is reduced to **2**·Cu^{I} by tris(2-carboxyethyl)phosphine. b) 2,9-Diphenyl-1,10-phenanthroline phosphoramidite (dpp vertex) used for in-strand DNA labeling. OMMTr = 4-monomethoxytrityl. c) AMBER local minimum energy structure of **2**·Cu^{I}. d) Formation and dynamic switching of **7**Cu^{I}_3 and **8**·Cu^{I}_3.

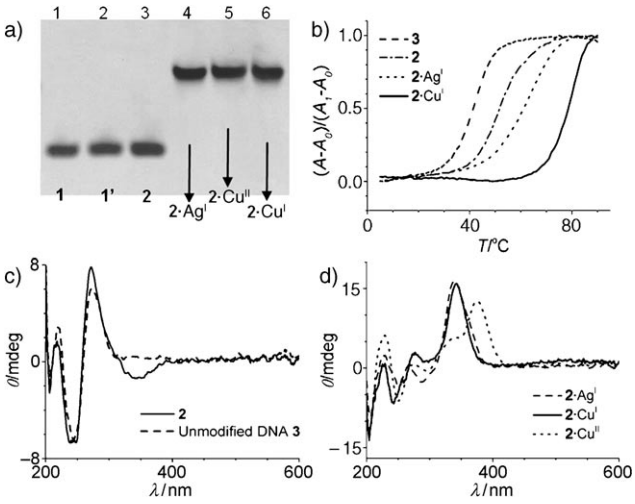

Figure 1. a) Denaturing polyacrylamide gel electrophoresis (PAGE). Lane 1: **1**, lane 2: **1′**, lane 3: **2**, lane 4: **2**·Ag^{I}, lane 5: **2**·Cu^{II}, lane 6: **2**·Cu^{I}. b) Melting temperature curves. Unmodified DNA **3**: $T_m = 43\,°C$, **2**: $T_m = 52\,°C$, **2**·Ag^{I}: $T_m = 64\,°C$, **2**Cu^{I}: $T_m = 80\,°C$. c) CD spectra of **2** and **3**. d) CD spectra of **2**·Ag^{I}, **2**·Cu^{I}, and **2**·Cu^{II}.

spectrum of double-stranded dpp–DNA **2** is similar to an unmodified B-DNA duplex **3** (Figure 1c).[18] However, after metal coordination, the CD spectrum changes significantly. Complexes **2**·Ag^{I} and **2**·Cu^{I}, both with d^{10} metals, show significant reduction in the positive B-DNA band and the appearance of a large positive peak at 342 nm, which dominates the spectrum. This peak coincides with a UV/vis transition typical of these metal complexes.[19,20] Previous reports have shown that attached chiral sugars can induce a right-handed helical twist of metal–bis(dpp) complexes, resulting in CD features that are similar to those obtained from **2**·Ag^{I} and **2**·Cu^{I}.[21] This finding is consistent with likely chirality transfer from the DNA duplex to the dpp_2–Cu^{I} unit, which induces a helical arrangement of the dpp ligands. Preliminary AMBER force-field calculations show a right-handed helical arrangement of the two dpp ligands in these metal–DNA junctions (i.e., following the right-handed B-DNA helix).[15] It is of note that this CD peak, which dominates the spectrum of the metal–DNA junction, arises from a single metal center which is only a minor part of the entire structure (one metal center per 10-mer DNA duplex).

The CD spectrum of the Cu^{II}–DNA junction **2**·Cu^{II} reveals two dominant positive bands, consistent with UV/vis bands of $[Cu(phen)_2]^{2+}$ (Figure 1d).[19,20] Interestingly, the copper–DNA junction can be cleanly and reversibly cycled between the +1 and +2 oxidation states. Addition of the reducing agent tris(2-carboxyethyl)phosphine (TCEP) completely reverts the CD spectrum of **2**·Cu^{II} into a spectrum identical to **2**·Cu^{I}. In turn, addition of I_2/H_2O to **2**·Cu^{I} restores the Cu^{II} CD bands.[15] This is one of the rare examples of transition metal–DNA systems that can cycle between two redox states (only ferrocene–DNA and ruthenium-bipyridine-acetylacetonate–DNA systems were previously reported).[22] The strong CD signatures associated with the metals in these junctions can be used as diagnostic peaks for both the nature of the metal and its specific oxidation state.

Transition metal–DNA structures have been used as probes of energy and charge transport,[4] sequence-specific nucleases,[5] and detection systems.[6] DNA has been metalated by reduction of metal ions around its backbone[7] and by

creation of "bases" that can serve as ligands.[8] DNA has also templated the assembly of organic modules through metal–salen complexes.[9] A few recent studies have attached inert transition metals to the ends of DNA duplexes to create 1D and 2D assemblies.[3] In contrast to these approaches, the DNA-templated method described herein creates a unique coordination environment, which is able to induce the normally labile d^{10} metals Cu^{I} (which is very unstable in water), Ag^{I}, and Cu^{II} to form highly stable metal–DNA junctions.

In addition to mononuclear metal–DNA units, this approach can readily generate multinuclear structures containing precisely positioned metals and DNA strands (Scheme 1d). Three building blocks (**4**, **5**, and **6**) were synthesized by solid-phase DNA protocols as before. Each of these contains three DNA regions separated by two dpp ligands. Two outer 10-mer DNA sequences work as template regions to mediate the assembly of a DNA triangle and to direct the metalation of the $(dpp)_2$ units (Scheme 1d). The three internal 15-mer sequences serve as single-stranded sides in the triangle and allow structural switching of this molecule with external agents (see below).

Self-assembly of the desired metalated triangle is highly efficient. Sequential hybridization of **4**, **5**, **6** shows quantitative formation of the dimer **4**:**5** and triangle **7** on native PAGE (Figure 2a, lanes 1–3). Addition of 3.3 equivalents Cu^{I} to metalate all three sites shows near quantitative product formation to give **7**·Cu^{I}_3 (Figures 2a and 3a). The CD spectrum of **7**·Cu^{I}_3 is similar to the mononuclear DNA junction **2**·Cu^{I} (Figure 2b). Denaturation of the DNA arms results in a single band of significantly lower mobility than **4**, **5**, and **6**, showing that **7**·Cu^{I}_3 is held together by metal coordination (Figure 3a, lane 5). To ascertain that **7**·Cu^{I}_3 is a fully tris-metallated closed triangle, we synthesized a monometallated dimer (**4**:**5**·Cu^{I}_2, Figure 3b, lane 1) and an open, bis-metallated trimer that does not have the proper sequence to cyclize (**9**·Cu^{I}_2, Figure 3b, lane 3) and showed the mobility of **7**·Cu^{I}_3 (Figure 3a, lane 2) to be distinct from either of these structures. It is of note that, unlike in previous studies,[1–3] the assembly of this cyclic structure is quantitative, and no oligomeric byproducts are formed. We believe this to be due to the presence of single-stranded, flexible sides in triangle **7**, which can relieve any strain that may arise from the cyclization of its three components.

Unlike previous methods in DNA nanotechnology, which typically yielded fully double-stranded constructs, the single-stranded sides of triangle **7**·Cu^{I}_3 allow its ready functionalization,[15] and impart it with dynamic character. Controlled structural switching is demonstrated by using specific DNA strands to reversibly compress and release this triangle, thus tuning the distance between two of the metal centers (Scheme 1d). Molecule **s1** possesses two regions that are complementary to two of the triangle sides (**4** and **5**) and separated by a short organic spacer (C_6). Addition of **s1** to **7**·Cu^{I}_3 can compress this structure and bring two metal corners close together, forming **8**·Cu^{I}_3 (Scheme 1d). In turn, addition of **s2**, which is fully complementary to **s1**, can remove **s1** and release the original triangle (Scheme 1d). Both events can be confirmed by native PAGE (Figure 2a, lanes 5 and 6).[15] Thus,

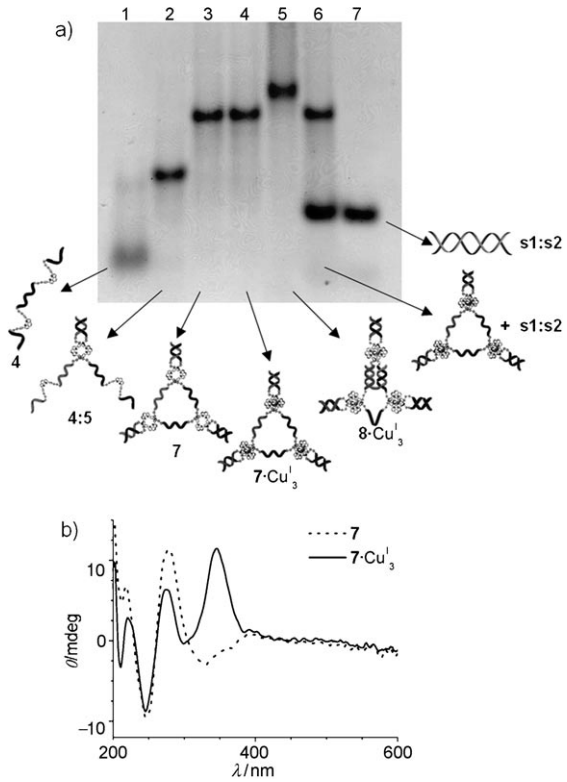

Figure 2. a) 16% Native PAGE. a) Lane 1: **4**, lane 2: **4**:**5**, lane 3: **7**, lane 4: **7**·Cu^{I}_3, lane 5: **8**·Cu^{I}_3, lane 6: addition of **s1** to **8**·Cu^{I}_3, forms **7**·Cu^{I}_3 + **s1**, lane 7: **s1**:**s2**. b) CD spectra of **7** and **7**·Cu^{I}_3.

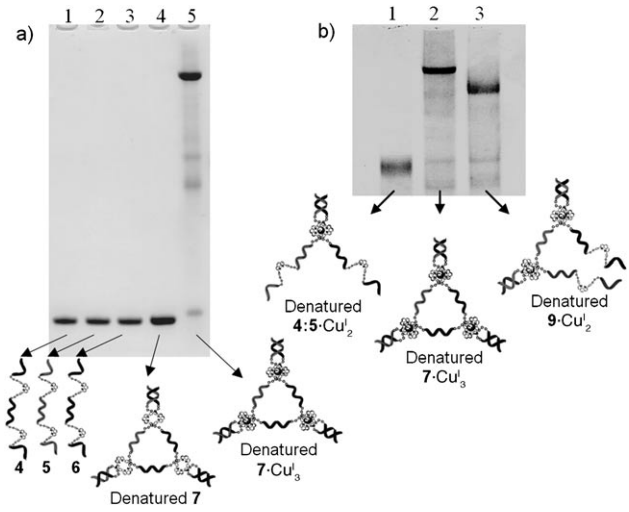

Figure 3. a) 14% Denaturing PAGE. Lane 1: **4**, lane 2: **5**, lane 3: **6**, lane 4: **7**, lane 5: **7**·Cu^{I}_3. b) 14% Denaturing PAGE. Lane 1: **4**:**5**·Cu^{I}_2, lane 2: **7**·Cu^{I}_3, lane 3: **9**·Cu^{I}_2.

copper–DNA triangle **7**·Cu^{I}_3 can undergo controlled and reversible structural switching with added DNA strands, resulting in modification of its geometry and modulation of the distance between its electroactive metal centers.

In summary, we have shown a new, DNA-templated method to create metal–DNA branch points which are electroactive and highly stable, thus allowing the introduction of normally kinetically labile transition metals into DNA junctions. Furthermore, this approach gives access to multi-

metallic structures, with metal complexes as their corners, single-stranded DNA as their sides, and multiple DNA double strands at their periphery. Ready and reversible structural changes of these metal–DNA nanostructures can be achieved using specific DNA strands and result in controlled modulation of the distance between the metal centers. Overall, the in-strand complexation of metals into DNA junctions allows for the potential of a large number of metals to be exploited in DNA nanoassembly, and the dynamic character of these metal–DNA architectures allows for real-time control of structure and metal–metal distances. Current efforts are focused on using these multimetallic structures as building blocks for 2D and 3D metal–DNA assemblies.

Received: August 14, 2007
Revised: November 16, 2007

Keywords: DNA · nanostructures · redox chemistry · self-assembly · transition metals

[1] Recent reviews: a) N. C. Seeman, *Nature* **2003**, *421*, 427 – 431; b) N. C. Seeman, *Methods Mol. Biol.* **2005**, *303*, 143 – 166; c) A. Condon, *Nat. Rev. Genet.* **2006**, *7*, 565 – 575; d) U. Feldkamp, C. M. Niemeyer, *Angew. Chem.* **2006**, *118*, 1888 – 1910; *Angew. Chem. Int. Ed.* **2006**, *45*, 1856 – 1876; e) K. V. Gothelf, T. H. LaBean, *Org. Biomol. Chem.* **2005**, *3*, 4023 – 4037; f) C. Lin, Y. Liu, S. Rinker, H. Yan, *ChemPhysChem* **2006**, *7*, 1641 – 1647; g) S. Pitchiaya, Y. Krishnan, *Chem. Soc. Rev.* **2006**, *35*, 1111 – 1121.

[2] DNA assemblies with organic vertices: a) L. H. Eckardt, K. Naumann, P. W. Matthias, M. Rein, M. Schweitzer, N. Windhab; G. v. Kiedrowski, *Nature* **2002**, *420*, 286; G. v. Kiedrowski, *Nature* **2002**, *420*, 286; b) J. Shi, D. E. Bergstrom, *Angew. Chem.* **1997**, *109*, 70 – 72; *Angew. Chem. Int. Ed. Engl.* **1997**, *36*, 111 – 113; c) M. Scheffler, A. Dorenbeck, S. Jordan, M. Wüstefeld, G. v. Kiedrowski, *Angew. Chem.* **1999**, *111*, 3513 – 3518; *Angew. Chem. Int. Ed.* **1999**, *38*, 3311 – 3315; d) M. S. Shchepinov, K. U. Mir, J. K. Elder, M. D. Frank-Kamenetskii, E. M. Southern, *Nucleic Acids Res.* **1999**, *27*, 3035 – 3041; e) F. A. Aldaye, H. F. Sleiman, *Angew. Chem.* **2006**, *118*, 2262 – 2267; *Angew. Chem. Int. Ed.* **2006**, *45*, 2204 – 2209; f) F. A. Aldaye, H. F. Sleiman, *J. Am. Chem. Soc.* **2007**, *129*, 13376 – 13377; g) F. A. Aldaye, A. Faisal, H. F. Sleiman, F. Hanadi, *J. Am. Chem. Soc.* **2007**, *129*, 4130 – 4131.

[3] a) D. Mitra, N. Di Cesare, H. F. Sleiman, *Angew. Chem.* **2004**, *116*, 5928 – 5932; *Angew. Chem. Int. Ed.* **2004**, *43*, 5804 – 5808; b) I. Vargas-Baca, D. Mitra, H. J. Zulyniak, J. Banerjee, H. F. Sleiman, *Angew. Chem.* **2001**, *113*, 4765 – 4768; *Angew. Chem. Int. Ed.* **2001**, *40*, 4629 – 4632; c) K. M. Stewart, L. W. McLaughlin, *J. Am. Chem. Soc.* **2004**, *126*, 2050 – 2057; d) K. M. Stewart, J. Rojo, L. W. McLaughlin, *Angew. Chem.* **2004**, *116*, 5932 – 5935; *Angew. Chem. Int. Ed.* **2004**, *43*, 5808 – 5811; e) J. S. Choi, C. W. Kang, K. Jung, J. W. Yang, Y.-G. Kim, H. Han, *J. Am. Chem. Soc.* **2004**, *126*, 8606 – 8607; f) S. M. Waybright, C. P. Singleton, K. Wachter, C. J. Murphy, U. H. F. Bunz, *J. Am. Chem. Soc.* **2001**, *123*, 1828 – 1833.

[4] a) E. M. Boon, J. K. Barton, *Curr. Opin. Struct. Biol.* **2002**, *12*, 320 – 329; b) M. E. Núñez, J. K. Barton, *Curr. Opin. Chem. Biol.* **2000**, *4*, 199 – 206; c) H. Weizman, Y. Tor, *J. Am. Chem. Soc.* **2002**, *124*, 1568 – 1569; d) D. J. Hurley, Y. Tor, *J. Am. Chem. Soc.* **2002**, *124*, 3749 – 3762.

[5] a) N. Carmi, S. R. Balkhi, R. R. Breaker, *Proc. Natl. Acad. Sci. USA* **1998**, *95*, 2233 – 2237; b) H. E. Moser, P. B. Dervan, *Science* **1987**, *238*, 645 – 650.

[6] Y. Lu, *Chem. Eur. J.* **2002**, *8*, 4588 – 4596.

[7] a) E. Braun, Y. Eichen, U. Sivan, G. Ben-Yoseph, *Nature* **1998**, *391*, 775 – 778; b) G. A. Burley, J. Gierlich, M. R. Mofid, H. Nir, S. Tal, Y. Eichen, T. Carell, *J. Am. Chem. Soc.* **2006**, *128*, 1398 – 1399.

[8] a) K. Tanaka, A. Tengeiji, T. Kato, N. Toyama, M. Shionoya, *Science* **2003**, *299*, 1212 – 1213; b) G. H. Clever, C. Kaul, T. Carell, *Angew. Chem.* **2007**, *119*, 6340 – 6350; *Angew. Chem. Int. Ed.* **2007**, *46*, 6226 – 6236.

[9] a) K. V. Gothelf, A. Thomsen, M. Nielsen, E. Clo, R. S. Brown, *J. Am. Chem. Soc.* **2004**, *126*, 1044 – 1046; b) J. L. Czlapinski, T. L. Sheppard, *J. Am. Chem. Soc.* **2001**, *123*, 8618 – 8619.

[10] a) B. Champin, P. Mobian, J.-P. Sauvage, *Chem. Soc. Rev.* **2007**, *36*, 358 – 366; b) N. Armaroli, *Chem. Soc. Rev.* **2001**, *30*, 113 – 124; c) C. O. Dietrich-Buchecker, J.-P. Sauvage, *Chem. Rev.* **1987**, *87*, 795 – 810; d) J.-P. Sauvage, C. O. Dietrich-Buchecker, *Molecular Catenanes, Rotaxanes and Knots*, Wiley-VCH, Weinheim, **1999**.

[11] C. Dietrich-Buchecker, J.-P. Sauvage, J. M. Kern, *J. Am. Chem. Soc.* **1989**, *111*, 7791 – 7800.

[12] a) B. C. Bales, T. Kodama, Y. N. Weledji, M. Pitie, B. Meunier, M. M. Greenberg, *Nucleic Acids Res.* **2005**, *33*, 5371 – 5379; b) S. Mahadevan, M. Palaniandavar, *Inorg. Chem.* **1998**, *37*, 3927 – 3934; c) J. M. Veal, R. L. Rill, *Biochemistry* **1991**, *30*, 1132 – 1140.

[13] a) C. Dietrich-Buchecker, J.-P. Sauvage, *Tetrahedron* **1990**, *46*, 503 – 512; b) K. S. Bang, M. B. Nielsen, R. Zubarev, J. Becher, *Chem. Commun.* **2000**, 215 – 216; c) M. Weck, B. Mohr, J.-P. Sauvage, R. H. Grubbs, *J. Org. Chem.* **1999**, *64*, 5463 – 5471.

[14] Untemplated complexation of Cu^{II} and Ag^{I} to dpp with a single DNA arm or Cu^{I}, Ag^{I}, Cu^{II} to dpp with two DNA arms was not possible. The exception was complexation of Cu^{I} to dpp with a single DNA arm.

[15] Please see the Supporting Information for more details.

[16] **2**·Cu^{II} does not have a distinct T_m owing to its dissociation upon heating.

[17] a) G. Bianké, V. Chaurin, M. Egorov, J. Lebreton, E. C. Constable, C. E. Housecroft, R. Häner, *Bioconjugate Chem.* **2006**, *17*, 1441 – 1446; b) M. Kalek, A. S. Madsen, J. Wengel, *J. Am. Chem. Soc.* **2007**, *129*, 9392 – 9400.

[18] A small additional negative peak at 350 nm that coincides with a dpp-centered UV/vis band indicates a small amount of chirality transfer from the DNA duplex to the dpp ligands in duplex.

[19] C. O. Dietrich-Buchecker, J.-P. Sauvage, J. M. Kern, *J. Am. Chem. Soc.* **1989**, *111*, 7791 – 7800.

[20] In its CD spectrum, **2**·Cu^{I} has a positive peak at 342 nm and **2**·Cu^{II} has a small positive peak at 341 nm and a large positive peak at 375 nm. The reported UV/vis spectrum of $[Cu(dpp)_2]^{+}$ has a peak at 331 nm, and $[Cu(dpp)_2]^{2+}$ has peaks at 300 and 360 nm.

[21] a) M. Yamamoto, M. Takeuchi, S. Shinkai, *Tetrahedron Lett.* **1998**, *39*, 1189 – 1192; b) C. R. Woods, M. Benaglia, F. Cozzi, J. S. Siegel, *Angew. Chem.* **1996**, *108*, 1977 – 1980; *Angew. Chem. Int. Ed. Engl.* **1996**, *35*, 1830 – 1833; c) evidence for positive couplet: 1) large first positive Cotton effect (CE) at around 340 nm, and a negative CE at lower wavelength that overlaps with B-DNA positive band; 2) first positve CE bands for **2**·Cu^{I}/**2**·Ag^{I}/**2**·Cu^{II} are all red-shifted from the corresponding UV/Vis bands.

[22] P. de-los-Santos-Álvarez, M. J. Lobo-Castanon, A. J. Miranda-Ordieres, P. Tunon-Blanco, *Anal. Bioanal. Chem.* **2004**, *378*, 104 – 118, and references therein.

